Scattering Analysis of a Millimeter-Wave Scalar Network Analyzer

JEFFREY B. KNORR, SENIOR MEMBER, IEEE

Abstract—**This paper presents the results of a scattering analysis of a millimeter-wave scalar network analyzer system. The results clearly indicate the way in which the individual system components contribute to calibration and measurement error. Procedures which minimize the calibration error for waveguide measurement systems are described, and the residual measurement uncertainty is quantified in a way which establishes the tightest possible bound on the measurement error.**

I. Introduction

OVER THE PAST several years, there has been considerable progress in the development of millimeter-wave components and systems. The development activity in the millimeter-wave bands has resulted in a demand for measurement systems. At microwave frequencies, both scalar and vector network analyzer systems have been available for some time. These network measurement systems are commercially available from several sources and have reached an advanced level of sophistication with regard to accuracy and automation. They are coaxial based and their performance is generally well understood. At millimeter-wave frequencies, the situation is far less satisfactory. Until recently, an individual with the need to make millimeter-wave network measurements faced the task of creating his own measurement system. Now, scalar millimeter-wave analyzer systems are available commercially from at least one source, so progress has been made with regard to hardware availability. However, millimeter-wave measurement systems are normally waveguide-based and it is difficult to determine the performance of these systems through reference to the existing literature on microwave systems.

The best source of information on the performance of microwave scalar network analyzer systems appears to be the literature available from the various manufacturers (see [1], for example). Such literature, however, tends to be slanted toward the use of particular equipment and emphasizes the use of coaxial components. Although many of the measurement system performance principles are independent of whether the hardware is coax or waveguide, it was found that the performance of a millimeter-wave scalar network analyzer could not be satisfactorily explained using results as they appear in the existing literature.

Manuscript received June 6, 1983; revised September 6, 1983. This work was supported in part by the Naval Postgraduate School Foundation Research Program.

The author is with the Department of Electrical Engineering, Naval Postgraduate School, Monterey, CA 93943.

The work described in this paper was motivated by the need to answer questions which arose during the development of an automated 60–90-GHz waveguide-based scalar network analyzer system. The questions related to system calibration and measurement uncertainties and their relationship to the characteristics of the individual components used to construct the system. Hence, the analyzer system was modeled as a multiport network and its response was determined through analysis using S-parameters. The purpose of the analysis was to explicitly relate the system response to the characteristics of the various components used in the system. The analysis has pointed the way to the best calibration procedures for waveguide-based systems and shows how measurement uncertainty may be quantified in a manner which permits the tightest possible bounds to be established for measurement error. The results presented here should be of considerable interest to those individuals faced with the problem of attempting to measure the insertion loss or return loss of a millimeter-wave network and to subsequently determine the measurement uncertainty.

II. Scalar Analyzer Analysis

A. System Description

A scalar millimeter-wave network analyzer consists of a signal source, directional couplers and detectors to sample incident and scattered waves, and a receiver to process the detector signals and display the results. If automated, the system will also have a computer which is interfaced with the signal source and receiver via a control bus. A typical system diagram is shown in Fig. 1. The objective is to use the measurement system to determine the insertion loss IL and return loss RL of a device under test (DUT). With the DUT in the forward direction (port A driven), the return loss at port A and the insertion loss from port A to port B are related to the scattering coefficients of the DUT by

$$RL_A = -10\log_{10}|S_{11}^{DUT}|^2 \tag{1a}$$

$$IL_{AB} = -10\log_{10}|S_{21}^{DUT}|^2. \tag{1b}$$

If the DUT is reversed, then we obtain

$$RL_B = -10\log_{10}|S_{22}^{DUT}|^2 \tag{1c}$$

$$IL_{BA} = -10\log_{10}|S_{12}^{DUT}|^2. \tag{1d}$$

Thus, the scalar measurement system provides data from

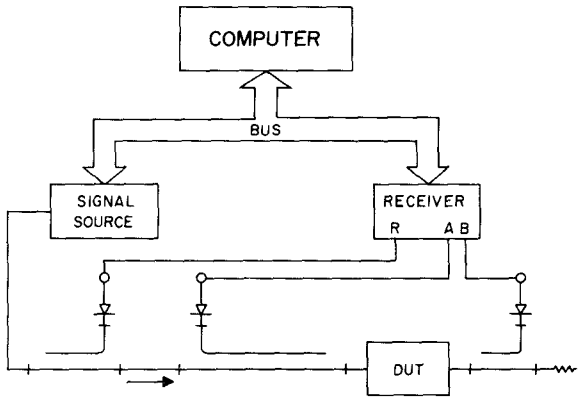

Fig. 1. Interconnection of millimeter-wave scalar network analyzer components and instruments.

which the magnitudes of the scattering coefficients of the DUT may be determined.

A more detailed diagram of the measurement system couplers is shown in Fig. 2. The three couplers will be referred to as the R, A, and B couplers since they provide samples of the incident (reference) signal, the signal scattered from port A of the DUT, and the signal scattered from port B of the DUT, respectively. The square-law detectors at coupler ports 3, 4, and 6 provide output signals directly proportional to the RF-signal power scattered to these three ports. The return loss is determined from the ratio V_A/V_R, while insertion loss is found from the ratio V_B/V_R. In an ideal system, these ratios would provide the desired quantities *IL* and *RL* directly. In practice, however, the results are corrupted by component imperfections. This makes it necessary first to calibrate the system and then to accept some uncertainty when a measurement is made.

The analysis which follows will identify the errors introduced by system component imperfections. It further indicates how calibration uncertainty may be eliminated and how measurement uncertainty may be quantified.

B. Return-Loss Measurement Analysis

Return loss is given by (1a) and (1c), which may be rewritten in the form

$$RL_k = -10\log_{10} P_k^-/P_k^+ \tag{2}$$

where P_k^- is the power scattered from port k of the DUT, and P_k^+ is the power incident on port k of the DUT. Samples of the incident and scattered waves are coupled to ports R and A, where they are applied to the square-law detectors which produce output voltages V_R and V_A, respectively. We are interested in the ratio of these voltages which may be expressed as

$$(V_A/V_R) = \text{const}\,(G_{T_{41}}/G_{T_{31}}) \tag{3}$$

where

$$G_{T_{qp}} = \frac{\text{power delivered to port } q}{\text{power available from source } p}.$$

As shown in Appendices A and B, the ratio of detector voltages may be expressed in terms of the scattering coefficients of the reflectometer bridge as

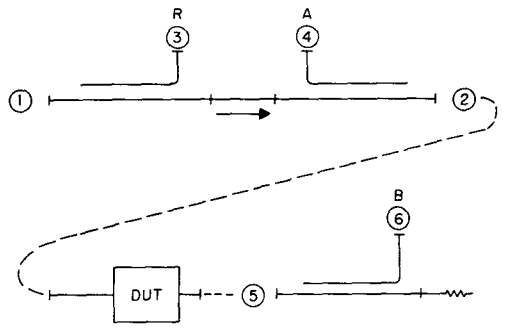

Fig. 2. Detailed diagram of measurement system directional couplers. Ports are identified for analysis purposes.

$$(V_A/V_R) = a^2\left|\frac{S_{41}}{S_{42}} + S_{21}(1+S_{22}\Gamma_{\text{in}})\Gamma_{\text{in}}\right|^2 \tag{4}$$

where a^2 is a constant, and Γ_{in} is the input reflection coefficient of the DUT and where it has been assumed that $|S_{22}\Gamma_{\text{in}}| \ll 1$. Further, it should be recognized that $|S_{21}| \approx 1$ and that $|S_{41}/S_{42}| \ll 1$ will be approximately equal to the directivity of the A coupler. However, the coupler directivity will always be an upper bound for $|S_{41}/S_{42}|$.

Before making an insertion-loss measurement, the system must be calibrated so that the 0-dB return-loss reference level is known. Equation (4) indicates that this may be accomplished using a sliding short. In this case, $\Gamma_{\text{in}} = e^{j\Phi}$ and, as the position of the short is varied, one obtains maximum and minimum readings (at each measurement frequency)

$$(V_A/V_R)^{1/2}_{\substack{\text{cal}\\ \max}} = a|S_{21}|(1+|S_{22}|)+\delta \tag{5a}$$

$$(V_A/V_R)^{1/2}_{\substack{\text{cal}\\ \min}} = a|S_{21}|(1-|S_{22}|)-\delta \tag{5b}$$

where

$$\delta = C|S_{41}/S_{42}| \qquad (-1 \leqslant C \leqslant +1). \tag{6}$$

If these readings are averaged, we obtain

$$(V_A/V_R)^{1/2}_{\substack{\text{cal}\\ \text{avg}}} = 1/2\left[(V_A/V_R)^{1/2}_{\substack{\text{cal}\\ \max}} + V_A/V_R)^{1/2}_{\substack{\text{cal}\\ \min}}\right] = a|S_{21}| \tag{7a}$$

which means that the correct *RL* reference level may be precisely located. We may also calculated

$$\frac{(V_A/V_R)^{1/2}_{\substack{\text{cal}\\ \max}} - (V_A/V_R)^{1/2}_{\substack{\text{cal}\\ \min}}}{2(V_A/V_R)^{1/2}_{\substack{\text{cal}\\ \text{avg}}}} = |S_{22}+\delta \tag{7b}$$

and this will be useful in evaluating the residual uncertainty when a measurement is made. $|S_{22}|$ is the equivalent of source mismatch, and it is determined from (7b) with uncertainty no greater than the A coupler directivity (see (6)).

The previous results have been derived assuming that a perfect sliding short is used to calibrate the system. If the

short is lossy, then its reflection coefficient will have a magnitude less than unity. The return-loss reference level in this case will be in error by an amount equal to the loss in decibels. For example, if the sliding short produces VSWR = 20, then $|\Gamma| = 0.905$ and the reference level will be 0.86 dB too low. All subsequent measurements referenced to this level would be in error by the same amount. Since waveguide losses increase dramatically in the millimeter-wave bands, this source of error should not be neglected.

Now suppose that a DUT is connected to port 2 of the A coupler. In this case, we have no control over the phase of the reflection from the input port of the DUT and we obtain

$$\frac{(V_A/V_R)^{1/2}_{\text{DUT}}}{(V_A/V_R)^{1/2}_{\substack{\text{cal}\\ \text{avg}}}} = \left| \frac{S_{41}}{S_{42}|S_{21}|} + \frac{S_{21}}{|S_{21}|}\Gamma_{\text{in}} + \frac{S_{21}}{|S_{21}|}S_{22}\Gamma_{\text{in}}^2 \right|. \quad (8a)$$

This may be written as

$$\frac{(V_A/V_R)^{1/2}_{\text{DUT}}}{(V_A/V_R)^{1/2}_{\substack{\text{cal}\\ \text{avg}}}} = |\Gamma_{\text{in}}| + C_1 \left| \frac{S_{41}}{S_{42}S_{21}} \right| + C_2|S_{22}||\Gamma_{\text{in}}|^2. \quad (8b)$$

The constants C_1 and C_2 lie in the interval $[-1,1]$ and depend upon the phases of the directivity and equivalent source mismatch error signal components relative to the signal reflected from the input of the DUT. Clearly, directivity and equivalent source mismatch error cause an uncertainty in the measurement of the DUT input-reflection coefficient. This uncertainty will vary with frequency and is dependent upon $|\Gamma_{\text{in}}|$ as well. As shown by (7b), $|S_{22}|$ may be found with small uncertainty at each measurement frequency during calibration. $|S_{41}/S_{42}|$ is not generally known as a function of frequency but is bounded from above by the coupler directivity D, which is specified by the manufacturer. Thus, we may express the detector voltage ratios in the form

$$\frac{(V_A/V_R)^{1/2}_{\text{DUT}}}{(V_A/V_R)^{1/2}_{\substack{\text{cal}\\ \text{avg}}}} = |\Gamma_{\text{in}}| \pm \Delta\Gamma_{\text{in}} \quad (8c)$$

where the worst case uncertainty $\Delta\Gamma_{\text{in}}$ is given by

$$\Delta\Gamma_{\text{in}} = D + |S_{22}||\Gamma_{\text{in}}|^2$$

if we assume $|S_{21}| \approx 1$.

The calibration and measurement data acquisition and the computation of measurement uncertainty as described above may be accomplished easily with an automated measurement system. During calibration, it is necessary to move a sliding short through a distance of at least one half a guide wavelength λ', so that the phase of the reflected signal varies through a full 360 degrees. An appropriate calibration algorithm would be one which searches for and stores the maximum and minimum values of (V_A/V_R) at each desired frequency as the short is moved a distance $\lambda'/2$ at the lowest frequency in perhaps 10 steps. After acquiring the DUT reflection data, an undistorted graph of return loss versus frequency with error bars may be generated by the computer. This is particularly attractive in the case of a millimeter-wave system since the reference level $a|S_{21}|$ in (7a) will exhibit a significant dependence on frequency. This occurs because the constant a is determined by the response of the detectors which currently have poor flatness and tracking in the millimeter bands. Poor source leveling also causes variations in detector output with frequency.

Fig. 2 shows an isolater, the purpose of which has not yet been addressed. The performance improvement which can be realized by using the isolator becomes clear only if one also analyzes the behavior of the system when the isolator is not present. Such an analysis has been carried out. The results show that the interaction among the DUT, source, and R detector (which occurs in that case) degrades measurement system accuracy. Since uncertainty is reduced and the analysis simplified when an isolator is included in the system, its use is recommended. This assumes that the VSWR of the isolator is approximately the same as that of the source.

The equivalent source mismatch $|S_{22}|$ is a major contributor to measurement uncertainty. It is therefore desirable to minimize $|S_{22}|$, if possible. By definition, S_{22} is the reflection coefficient seen looking into port 2 of the reflectometer when ports 1, 3, and 4 are terminated in matched loads. The magnitude of this reflection may be estimated from the VSWR's of the isolator and the A coupler. The worst case occurs when the signal components reflected by the coupler and the isolator are in phase. If the VSWR's of the coupler and isolator are sufficiently small, the upper bound on $|S_{22}|$ may be approximated by

$$|S_{22}| \leq \frac{S_c - 1}{S_c + 1} + \frac{S_I - 1}{S_I + 1} \quad (9)$$

where S_I is the isolator VSWR (maximum), and S_c is the coupler VSWR (maximum). Thus, measurement uncertainty may be minimized by using an isolator and the A coupler with the lowest possible upper bound on VSWR.

There are two remaining observations which are worthy of comment. The first relates to the reflection coefficients Γ_{D3} and Γ_{D4} of the R and A coupler detectors. Although these reflection coefficients enter into the determination of the gains $G_{T_{41}}$ and $G_{T_{31}}$, the final result is independent of detector VSWR. At any fixed frequency, the effects of detector VSWR are the same during both calibration and measurement and thus disappear through cancellation of the factor a which appears in both (4) and (7a). Lastly, it should be noted that the measured DUT input reflection coefficient is given by

$$\Gamma_{\text{in}} = S_{11}^{\text{DUT}} + \frac{S_{12}^{\text{DUT}}S_{21}^{\text{DUT}}\Gamma_L}{1 - S_{22}^{\text{DUT}}\Gamma_L} \quad (10)$$

where Γ_L is the reflection coefficient of the load terminating the DUT. To evaluate the return loss (see (1)), $|S_{11}^{\text{DUT}}|$ is required. Equation (10) shows that $|\Gamma_{\text{in}}| = |S_{11}^{\text{DUT}}|$ only if $|\Gamma_L| = 0$. Therefore, the best possible load should be placed on port B of the DUT when measuring $|\Gamma_{\text{in}}|$ at port A, and

vice versa. If the DUT is terminated in the B coupler so that return-loss and insertion-loss data may be simultaneously acquired and displayed, then the B coupler VSWR will cause additional uncertainty in $|S_{11}^{\mathrm{DUT}}|$. Therefore, to achieve the lowest uncertainty, the unexcited port of the DUT should be terminated in a waveguide matched load. Such a load has a VSWR, which is significantly lower than that of a directional coupler. Additionally, if a sliding load is used, the error due to load reflection may be averaged out in the same way that the equivalent source mismatch error is averaged out during the return-loss calibration procedure (see (5), (7)).

C. Insertion-Loss Measurement Analysis

Insertion loss is given by (1b) and (1d) and may be put in the form

$$IL_{kq} = -10_{\log_{10}} P_q^- / P_k^+ \tag{11}$$

where P_q^- is the power scattered from port q of the DUT, and P_k^+ is the power incident on port k of the DUT. All ports are terminated in the load impedance Z_0, except port k which is driven by a source with impedance Z_0. For this measurement, the network is terminated in the B coupler and samples of the incident and scattered waves are coupled to ports R and B, respectively. The square-law detectors at these ports produce output voltages V_B and V_R. The ratio of these voltages is given by

$$(V_B/V_R) = \mathrm{const}\left(G_{T_{61}}/G_{T_{31}}\right). \tag{12}$$

As shown in the Appendix, the ratio of these detector voltages may be expressed in terms of the scattering coefficients of the DUT as

$$(V_B/V_R)^{1/2} = d\left[\frac{|S_{21}^{\mathrm{DUT}}|}{|(1-S_{11}^{\mathrm{DUT}}\Gamma_s')(1-S_{22}^{\mathrm{DUT}}\Gamma_L') - S_{12}^{\mathrm{DUT}}S_{21}^{\mathrm{DUT}}\Gamma_s'\Gamma_L'|}\right] \tag{13}$$

where d is a constant, Γ_s' is the reflection coefficient seen looking into port 2 of the A coupler, and Γ_L' is the reflection coefficient seen looking into port 5 of the B coupler. In this case, the measurement system is calibrated by placing the A and B couplers directly together, i.e., using a zero length through section, in which case

$$S_{11}^{\mathrm{DUT}} = S_{22}^{\mathrm{DUT}} = 0 \tag{14a}$$

$$S_{21}^{\mathrm{DUT}} = S_{12}^{\mathrm{DUT}} = 1. \tag{14b}$$

Thus

$$(V_B/V_R)_{\mathrm{cal}}^{1/2} = \frac{d}{|1-\Gamma_s'\Gamma_L'|} \tag{15}$$

and the correct reference level d (0-dB insertion loss) is located with uncertainty equal to $\pm d|\Gamma_s'\Gamma_L'| \ll d$. In principle, this uncertainty could be removed by placing a variable length through section between the A and B couplers. An averaging of maximum and minimum readings as the through section length varied would then produce a correct result as in the case of return loss. In practice, however, a variable length waveguide section is not currently available, so this procedure cannot be implemented. Since the uncertainty is reduced by making $|\Gamma_s'|$ and $|\Gamma_L'|$ as small as possible, it is clear that better accuracy can always be obtained by removing the A coupler during calibration (and measurement) for insertion loss. When this is done, $|\Gamma_s'|$ is determined solely by the isolator VSWR.

The worst case uncertainty in the location of the reference level may be calculated from the system component specifications. With the A coupler in the system, the reflection coefficients Γ_s' and Γ_L' seen looking into the A and B couplers are given by

$$\Gamma_s' = S_{22} + \frac{S_{24}S_{42}\Gamma_{D4}}{1-S_{22}\Gamma_{D4}} \tag{16a}$$

$$\Gamma_L' = S_{55} + \frac{S_{65}S_{56}\Gamma_{D6}}{1-S_{66}\Gamma_{D6}}. \tag{16b}$$

In each case, one coupler port is effectively terminated (A coupler by isolator, B coupler by load) so that they appear to the DUT-like 2-port networks terminated in loads Γ_{D4} and Γ_{D6}, respectively. When written in this form, it can be seen that the best accuracy will be obtained if couplers and detectors with the lowest possible VSWR's are used. Since millimeter-wave detectors frequently have high VSWR's, it will generally be beneficial to use an isolator ahead of each detector. This assumes, of course, that the VSWR of the isolator is substantially lower than that of the detector. In either case, the reflection from the secondary arm of the coupler is reduced by the coupling factor (typically 10 dB). Suppose, for example, that the specifications of the various components are as follows:

B & A coupler primary arm, VSWR 1.10
B & A coupler secondary arm, VSWR 1.20
B & A coupler coupling factor = 10 dB
Isolator, VSWR 1.50
Load, VSWR 1.05
Detector, VSWR 3.

The worst case values of $|\Gamma_L'|$ and $|\Gamma_s'|$ in this case are approximately given by

$$|\Gamma_s'| \leq 0.05 + 0.20 + 0.05 = 0.30 \tag{17a}$$

$$|\Gamma_L'| \leq 0.05 + 0.02 + 0.05 = 0.12 \tag{17b}$$

when the detectors are not preceeded by isolators. If isolators are used ahead of the detectors, then

$$|\Gamma_s'| \leq 0.27 \tag{18a}$$

$$|\Gamma_L'| \leq 0.09. \tag{18b}$$

Using (15), (17), and (18), we find that the worst case uncertainty is ± 0.32 dB without isolators, while with isolators it is reduced to ± 0.21 dB. If the A coupler is removed from the system, then the equivalent source mismatch is reduced to $|\Gamma_s'| \leq 0.2$. The worst case uncertainty in the location of the 0-dB reference level for insertion-loss mea-

surements is correspondingly reduced to ± 0.15 dB, assuming an isolator is used ahead of the B coupler detector.

The uncertainty may be bounded more tightly if during the insertion-loss calibration run the return loss of the B coupler is measured. This will establish the value of $|\Gamma_L'|$. During the return-loss calibration run, the value of $|S_{22}|$ is found. Thus, $|\Gamma_s'| \leqslant |S_{22}| + C|\Gamma_{D4}|$ when the A coupler coupler is in the system (C is the power coupling factor). If the A coupler is removed from the system

$$|\Gamma_s'| \leqslant (S_I - 1)/(S_I + 1).$$

For either situation, the calibration uncertainty

$$20_{\log_{10}}\left(1 + |\Gamma_s'\Gamma_L'|\right)$$

is reduced since $|\Gamma_L'|$ is known from direct measurement at each frequency of interest.

Now suppose that a DUT is placed between the A and B couplers. We then obtain

$$\frac{(V_A/V_R)_{\text{DUT}}^{1/2}}{(V_B/V_R)_{\text{cal}}^{1/2}} = \left[\frac{|1 - \Gamma_s'\Gamma_L'|}{|(1 - S_{11}^{\text{DUT}}\Gamma_s')(1 - S_{22}^{\text{DUT}}\Gamma_L') - S_{12}^{\text{DUT}}S_{21}^{\text{DUT}}\Gamma_s'\Gamma_L'|}\right]|S_{21}^{\text{DUT}}|.$$

The measurement error clearly depends upon the scattering coefficients of the DUT and the quantities Γ_s', Γ_L'. One has no control over the scattering coefficients of the DUT since this is designed to meet requirements having nothing to do with measurement error. Thus, the desirability of minimizing $|\Gamma_s'|$ and $|\Gamma_L'|$ through use of the highest quality components is further emphasized. To reiterate, the lowest possible coupler, isolator, and detector VSWR's are required to minimize both $|\Gamma_s'|$ and $\Gamma_L'|$. If the accuracy achieved with the best available components is not satisfactory, then E–H tuners may be used to further reduce $|\Gamma_s'|$ and $|\Gamma_L'|$ to negligibly small values. Retuning is required at each frequency, however, so this negates the use of an automatic system.

Equation (19) shows that the uncertainty in the measurement of $|S_{21}^{\text{DUT}}|$ is determined by the bracketed factor by which it is multiplied. In an automated system, error bars can be placed easily on the graph of insertion loss by evaluating the bracketed term to find the maximum and minimum values. The determination of bounds on $|\Gamma_s'|$ and $|\Gamma_L'|$ was discussed previously. The S_{ij}^{DUT} are the measured scattering coefficients of the DUT. Thus, this evaluation is straightforward. Again, the use of a computer to graph the result is very advantageous, as it eliminates the distortion which occurs due to detector and sweeper response when calibration and measurement sweeps are displayed using analog hardware without any storage normalization.

III. Results

The analytical results presented in the previous sections have been verified experimentally using an automated measurement system covering the 60–90-GHz band. The major components of the measurement system are a solid-state programmable sweep oscillator, a swept amplitude display device, and a desktop computer interconnected as indicated in Fig. 1. The remainder of the system consists of directional couplers, an isolator, and detectors interconnected as shown in Fig. 2. The computer software permits calibration and measurement data to be rapidly acquired for either insertion-loss or return-loss measurements. The measurement data are then plotted along with curves indicating the measurements uncertainty. These curves represent the tightest possible bounds on measurement uncertainty; points are computed at each test frequency. Some typical results are presented and discussed below.

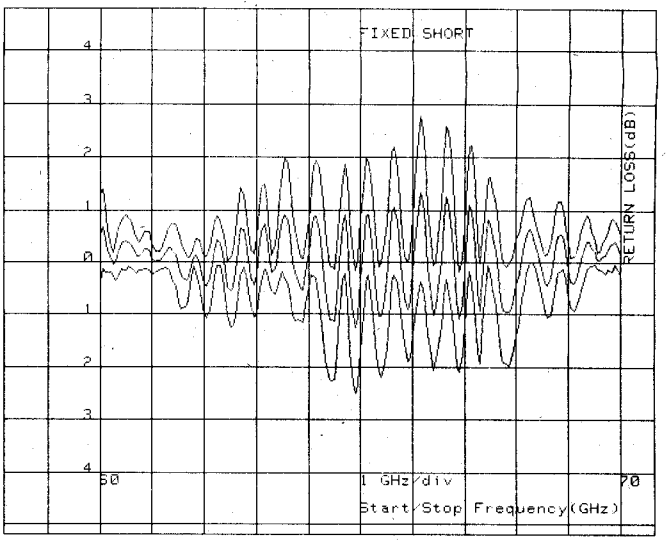

Fig. 3. Return loss versus frequency for a WR(12) fixed waveguide short.

A. Fixed Short

The return loss of a fixed waveguide short is of interest because the correct value of the return loss is known to be precisely 0 dB. It may thus be used to check the performance of the measurement system. The center curve in Fig. 3 shows the measured return loss for a WR (12) waveguide short. Notice that the return loss oscillates about the correct value of 0 dB as the frequency is varied. This oscillation is caused by the interference between the signal reflected from the short and the error signal component due to equivalent source mismatch. This represents a worst case situation since the reflection coefficient of the short is $|\Gamma| = 1$. For a load of unknown return loss, it is this error which introduces uncertainty into the measurement.

The upper and lower curves in Fig. 3 bound the measurement uncertainty. The correct value of return loss, 0 dB in this case, should always be between these two curves. It can be seen that this is generally the case, although there are several points where the upper bound dips a few tenths of a decibel below the 0-dB level. This small error is consistent with our use of 10 positions of the sliding short for calibration. The error results from the failure of the calibration algorithm to determine $|S_{22}|$ precisely. The error may be reduced by using more positions of the sliding short. Also evident in Fig. 3 is the variation of the uncer-

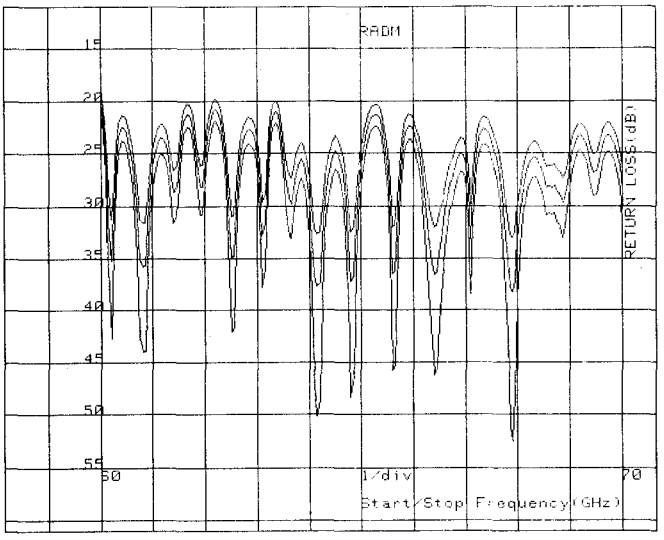

Fig. 4. Return loss versus frequency for a WR(12) broad-band detector mount.

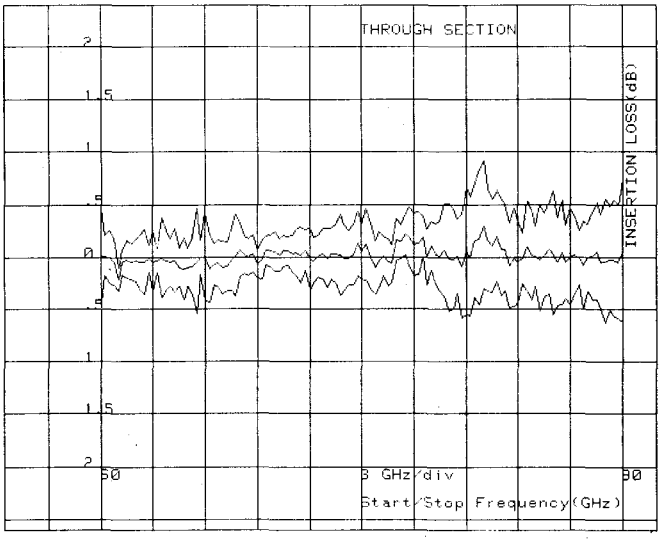

Fig. 5. Insertion loss versus frequency for a WR(12) waveguide through section 1.

tainty with frequency. Here, the uncertainty is less near the edges of the band than it is at the center. Thus, the uncertainty near the edges of the band has been reduced considerably relative to the bound computed using the worst case equivalent source VSWR.

B. Detector Mount

A second example of a return-loss measurement is shown in Fig. 4 which presents the data obtained for a detector. The measured return loss is in the range 20–40 dB over the frequency band 60–70 GHz. At this level, the source mismatch is less important than the A coupler directivity error. Since the A coupler directivity was >40 dB ($D \leqslant 0.01$) in our system, there is considerable uncertainty if the measured return loss is in the vicinity of 40 dB. This can be seen clearly in Fig. 3.

C. Through Section

The insertion loss of a through section is of interest because the correct value of the insertion loss is known to be 0 dB. It may therefore be used to check measurement system performance in the same manner as with the short. The measured return loss of a through section is shown in Fig. 5 along with the bounds on uncertainty. The measured insertion loss is within ± 0.3 dB of the correct value (0 dB) over the 60–90-GHz frequency range shown in the figure. The correct value of insertion loss also lies within the computed range of uncertainty delineated by the curves above and below the curve of measured insertion loss except at 61 GHz. At this frequency, a drop in the measured insertion loss has pulled the upper bound on the uncertainty below the 0-dB level to -0.1 dB. This anomaly is believed due to a small change in the output power level of the source between calibration and measurement at that frequency. Overall, insertion loss uncertainty is seen to be considerably less than was the case for return-loss measurements. This is in agreement with the results predicted by the model.

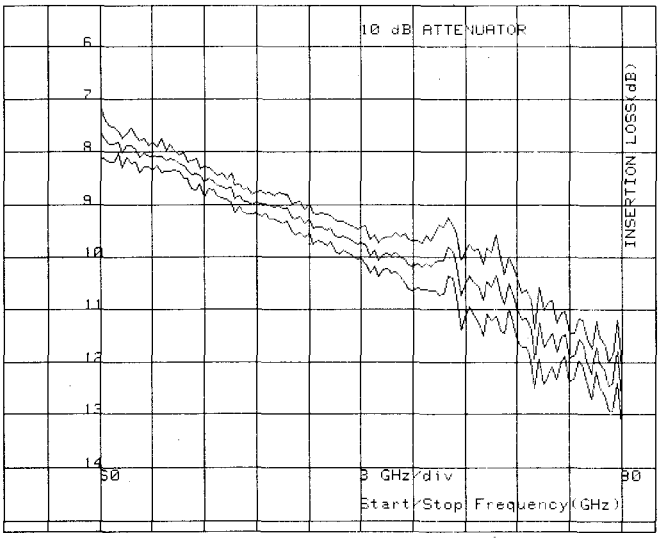

Fig. 6. Insertion loss versus frequency for a WR(12) waveguide attenuator.

D. Calibrated Attenuator

As a last example, Fig. 6 shows the measured insertion loss of a WR (12) calibrated variable attenuator over the 60–90-GHz band. This attenuator was supplied from the manufacturer with a calibration curve at 75 GHz, and the micrometer was set accordingly for 10 dB of attenuation. The measured insertion loss varied ± 2.5 dB over the frequency band, but was indeed measured to be 9.74 ± 0.3 dB at 75 GHz.

IV. Conclusions

This paper has presented a scattering analysis of a waveguide-based millimeter-wave scalar network analyzer system. The results of this analysis clearly indicate the relationship between system component specifications and the performance of the entire measurement system. These results may be summarized as follows.

1) The use of a (perfect) waveguide sliding short permits the correct 0-dB return-loss reference level to be found precisely. Losses in the short will cause an error equal to the decibel value of the losses in the short.

2) The use of a sliding short permits the equivalent source mismatch $|S_{22}|$ to be determined.

3) The equivalent source mismatch $|S_{22}|$ is determined by the VSWR's of the A coupler and isolator so these components should have the lowest possible VSWR's.

4) The measured equivalent source mismatch $|S_{22}|$ and the known A coupler directivity may be used to compute the uncertainty of return loss at each measurement frequency. Measurement of $|S_{22}|$ permits the tightest possible bounds on the measurement error to be established.

5) The use of an isolator between the R and A couplers improves system accuracy (and simplifies system analysis) by eliminating interaction between the R detector and the DUT.

6) The accuracy of return-loss measurements is not affected by the R and A detector VSWR.

7) To obtain the best possible accuracy when measuring return loss, the DUT should be terminated in a matched waveguide load, not the B coupler.

8) The correct 0-dB insertion-loss reference level could be found precisely if a variable length through section were available. Without one, the uncertainty is

$$10\log_{10}\left(1 \pm |\Gamma_s'\Gamma_L'|\right) \text{ dB}.$$

9) $|\Gamma_s'|$ and $|\Gamma_L'|$, the effective source and load reflection coefficients seen by the DUT, determine the uncertainty of an insertion-loss measurement. These quantities may be determined from calibration and measurement data, and thus error limits can be established.

10) $|\Gamma_s'|$ and $|\Gamma_L'|$ depend upon the VSWR's of the A and B couplers, A and B detectors, and the isolator. These components should have the lowest possible VSWR's if the insertion-loss measurement uncertainty is to be minimized. If low-VSWR isolators are placed ahead of high-VSWR detectors, the system insertion-loss measurement uncertainty will be reduced. The uncertainty may be reduced further if the A coupler is removed from the system when insertion loss is measured.

11) $|\Gamma_s'|$ and $|\Gamma_L'|$ may be reduced by using E–H tuners at spot frequencies to achieve higher accuracy. Mechanical tuners cannot be used in an automatic system, however, since retuning is necessary at each frequency.

12) The use of unnecessary components (such as waveguide switches) should be avoided since they will degrade system performance.

13) The use of a computer to control instruments and graph results is very desirable. Distortion due to source leveling and detector flatness can be removed and error limits can be computed and displayed.

The methods that are proposed here for determining measurements uncertainty result in the tightest possible bounds on the error. Calibration and measurement data are used to achieve this. Simple use of component specifications alone would result in considerably looser bounds on error.

The model discussed in this paper does not account for instrumentation errors. Errors of this type may occur due to the following: 1) signal source harmonics; 2) changes in signal source frequency or output power level between calibration and measurement; 3) non-square law operation of detectors; 4) nonlinear amplification of detected signals. These are errors that will depend upon the specific hardware implementation of the measurement system, but they should not be overlooked, particularly since millimeter-wave hardware is not yet mature.

Overall, the results presented here should bring the important features of measurement system response more clearly into view. The analysis should therefore be useful to those individuals concerned with scalar measurement of millimeter-wave network scattering coefficients.

Appendix A
Return-Loss Analysis

With reference to Fig. 2, the R coupler, A coupler, and isolator will be considered as a 4-port network. The behavior of this network may be determined from the network scattering equations. It will be assumed that $S_{14} = S_{12} = S_{34} = S_{32} = 0$ since these coefficients produce terms which are small in comparison to those retained. Likewise, $S_{43} \approx 0$ and will be neglected. Ports 3 and 4 are terminated with detectors having reflection coefficients Γ_{D3} and Γ_{D4}, respectively. If port 2 is terminated in a DUT having reflection coefficient Γ_{in}, then the scattering equations take the form

$$b_1 = S_{11}a_1 + S_{13}\Gamma_{D3}b_3 \tag{A1a}$$

$$b_2 = S_{21}a_1 + S_{22}\Gamma_{\text{in}}b_2 + S_{23}\Gamma_{D3}b_3 + S_{24}a_4 \tag{A1b}$$

$$b_3 = S_{31}a_1 + S_{33}\Gamma_{D3}b_3 \tag{A1c}$$

$$b_4 = S_{41}a_1 + S_{42}\Gamma_{\text{in}}b_2 + S_{44}a_4. \tag{A1d}$$

Using (A1a) and (A1c), it follows immediately that the transducer power gain from port 1 to port 3 is

$$G_{T31} = \frac{|S_{31}|^2\left(1-|\Gamma_s|^2\right)\left(1-|\Gamma_{D3}|^2\right)}{|(1-S_{11}\Gamma_s)(1-S_{33}\Gamma_{D3}) - S_{31}S_{13}\Gamma_{D3}\Gamma_s|^2} \tag{A2}$$

where Γ_s is the source reflection coefficient. By further manipulation of (A1), we can obtain

$$b_1 = (S_{11})a_1 \tag{A3a}$$

$$b_4 = \left(S_{41} + \frac{S_{42}S_{21}\Gamma_{\text{in}}}{(1-S_{22}\Gamma_{\text{in}})}\right)a_1 + S_{44}a_4. \tag{A3b}$$

(One term has been dropped from each of the bracketed coefficients because it is much smaller than the terms retained.) Using these equations, we obtain the transducer power gain from port 1 to port 4, which is

$$G_{T41} = \frac{\left|S_{41} + \frac{S_{42}S_{21}\Gamma_{\text{in}}}{(1-S_{22}\Gamma_{\text{in}})}\right|^2\left(1-|\Gamma_s|^2\right)\left(1-|\Gamma_{D4}|^2\right)}{|(1-S_{11}\Gamma_s)(1-S_{44}\Gamma_{D4})|^2}. \tag{A4}$$

Equations (A4) and (A2) have been obtained by considering the port pairs, 1–3 and 1–4, one at a time so that the 2-port transducer power gain expression can be used.

The A and R detectors will each produce an output voltage proportional to the power delivered to their respective ports. In general, the constant of proportionality will differ from one detector to another. Thus

$$(V_A/V_R) = \text{const}\left(G_{T_{41}}/G_{T_{31}}\right). \tag{A5}$$

Further, $G_{T_{31}}$ is independent of the DUT and is constant, while in (A4) all terms involving source and detector reflection coefficients are also constant. Equation (A5) therefore assumes the relatively simple form

$$(V_A/V_R) = a^2\left|\frac{S_{41}}{S_{42}} + \frac{S_{21}\Gamma_{\text{in}}}{(1-S_{22}\Gamma_{\text{in}})}\right|^2. \tag{A6}$$

Normally, $S_{22}\Gamma_{\text{in}} \ll 1$ so that A(6) may be rewritten as

$$(V_A/V_R) = a^2\left|\frac{S_{41}}{S_{42}} + S_{21}(1+S_{22}\Gamma_{\text{in}})\Gamma_{\text{in}}\right|^2. \tag{A7}$$

Appendix B
Insertion-Loss Analysis

Again referring to Fig. 2, we see that when a DUT is inserted into the measurement system it sees an effective source reflection coefficient Γ_s' looking into port 2, and an effective load reflection coefficient Γ_L' looking into port 5. The transducer power gain for the DUT is

$$G_T^{(\text{DUT})} = \frac{|S_{21}^{\text{DUT}}|^2\left(1-|\Gamma_s'|^2\right)\left(1-|\Gamma_L'|^2\right)}{\left|\left(1-S_{11}^{\text{DUT}}\Gamma_s'\right)\left(1-S_{22}^{\text{DUT}}\Gamma_L'\right)-S_{12}^{\text{DUT}}S_{21}^{\text{DUT}}\Gamma_s'\Gamma_L'\right|^2}. \tag{A8}$$

The source is isolated and the power available at port 2 is some constant fraction of the power available from the source driving port 1. Similarly, some constant fraction of the power delivered to port 5 appears at port 6 to drive the B detector. Therefore, the transducer power gain from port 1 to port 6 G_{T61} is given by

$$G_{T61} = b^2 G_T^{(\text{DUT})} \tag{A9}$$

where b^2 is a constant.

Following the same arguments as in the previous section, the ratio of detector voltages may be written as

$$(V_B/V_R) = \text{const}\left(G_{T61}/G_{T31}\right) \tag{A10}$$

or

$$(V_B/V_R) = d^2\frac{|S_{21}^{\text{DUT}}|^2}{\left|\left(1-S_{11}^{\text{DUT}}\Gamma_s'\right)\left(1-S_{22}^{\text{DUT}}\Gamma_L'\right)-S_{12}^{\text{DUT}}S_{21}^{\text{DUT}}\Gamma_s'\Gamma_L'\right|^2}. \tag{A11}$$

Acknowledgment

The author wishes to acknowledge the contributions of Lt. C. Shultheis, USN, Lt. G. Leoussis, and Lt. E. Gatsos, Hellenic Navy, and V. McCullough, Naval Postgraduate School. All have assisted with system integration, software development, and laboratory verification of analytical results. They persisted through a long series of software problems and hardware failures.

References

[1] "High frequency swept measurements," Application Note 183, Hewlett-Packard, Palo Alto, CA, May 1975.

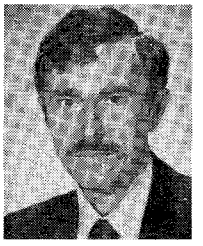

Jeffrey B. Knorr (S'68–M'71–SM'81) was born in Lincoln Park, NJ, on May 8, 1940. He received the B.S. and M.S. degrees in electrical engineering from Pennsylvania State University, University Park, PA, in 1963 and 1964, respectively, and the Ph.D. degree in electrical engineering from Cornell University, Ithaca, NY, in 1970.

From 1964 to 1967, he served with the U.S. Navy. In September 1970, he joined the faculty of the Naval Postgraduate School, Monterey, CA, where he currently holds the rank of Professor in the Department of Electrical Engineering and is the Faculty Director of the Microwave Laboratory. He is also a member of the Electronic Warfare Academic Group and the Space Systems Academic Advisory Committee. These groups are responsible for the administration of interdisciplinary programs in Electronic Warfare and Space Systems at the Naval Postgraduate School.

Dr. Knorr is a member of Sigma Xi and the Association of Old Crows.